Cell Tissue Res (1995) 279:149–167

Cell & Tissue Research

Initial enamel crystals are not spatially associated with mineralized dentine

Thomas G.H. Diekwisch*, Brett J. Berman, Steven Gentner, Harold C. Slavkin

Center for Craniofacial Molecular Biology, School of Dentistry, University of Southern California, 2250 Alcazar Street, CSA/105, Los Angeles, CA 90033, USA

Received: 13 October 1993 / Accepted: 28 June 1994

Abstract. During epithelial-mesenchymal interactions associated with mammalian tooth development, epithelially-derived and mesenchymally-derived extracellular matrix molecules form a discrete dentine-enamel junction. The developmental and molecular processes required to form this junction are not known. To address this problem we designed studies to test the hypothesis that ectodermally-derived epithelial cells synthesize and secrete enamel proteins which function to nucleate and regulate the growth of enamel calcium phosphate crystals. Initial enamel crystals were detected separate from the adjacent dentine. Electron-microprobe analyses revealed that early enamel crystals were octacalciumphosphate or tricalciumphosphate rather than hydroxyapatite. Thereafter, enamel crystals became confluent with the adjacent, albeit significantly smaller hydroxyapatite crystals associated with mineralized dentine. Therefore, we interpret our data to indicate that de novo enamel crystal nucleation and growth are independent from the mineralization processes characterized for dentine. We further argue that gene expression of enamel protein appears to have a constitutive function during early enamel formation and that supramolecular aggregates of amelogenin and enamelin provide the microenvironment for the nucleation and crystal growth of the initial enamel matrix.

Key words: Enamel – Tooth development – High-voltage electron-microscopy – 3-D reconstruction – Mouse

Introduction

Enamel is an extracellular product of ectodermally-derived epithelial cells which has 4 distinguishing characteristics: (i) the organic matrix consists of enamelins and amelogenins; (ii) the apatite crystallites are very much larger than those found in other vertebrate mineralized tissues (e.g. bone, calcifying cartilage, cementum, and dentine); (iii) the organic matrix is free of collagen; and (iv) enamel when mineralized is essentially 99.9% mineral. Enamel is the tooth-covering tissue found in adult amphibian, reptilian, and mammalian teeth. The appearance of long and organized calcium hydroxyapatite (HAP) crystals during vertebrate tooth evolution may be correlated with the introduction of amelogenins into the protein mixture of the forming enamel matrix. Simultanously, novel mechanisms for growth patterns of crystals may have been created. In the developing mouse molar, several mechanisms for nucleation and growth of enamel crystals may be present. These reflect Haeckel's law of ontogenesis replicating phylogenic development (Haeckel 1866).

In this report, we provide results from studies designed to test the hypothesis that in the mouse molar, nucleation and growth of enamel crystals are independent of apatite crystal nucleation and growth in the dentine. To test this hypothesis, we re-investigated the initial formation of the dentine-enamel junction (DEJ) in developing molar tooth organs in vivo and in vitro using serumless medium (Yamada et al. 1980; Bringas et al. 1987; Evans et al. 1988), and analyzed the spatial position of the first enamel crystals to form in relationship to the mineralizing dentine matrix. Initial enamel crystals, surrounded by an electron-dense stippled organic matrix, were first observed not to be connected to forming dentine crystals within mantle dentine. These enamel crystals had Ca/P ratios indicative of octacalciumphosphate (OCP) or tricalciumphosphate (TCP), but not of hyroxyapatite (HAP). Initial enamel formed as clusters of discrete TCP or OCP crystals independent from dentine HAP. The initial enamel mineral phases were different from those characteristic of adjacent dentine HAP. In later stages, enamel crystals had Ca/P ratios indicative of HAP, and then appeared as continuous with dentine HAP crystals. These results suggest that initial nucleation of enamel crystals occurs separately from the presence of mineralized dentine and thereafter becomes contiguous with the mineralized dentine.

* *Present address:* Department of Biomedical Sciences, Baylor College of Dentistry, P.O. Box 660667, Dallas, TX 75266-0677, USA

Correspondence to: H.C. Slavkin

Materials and methods

Molar dissection and organ culture

Newborn (day 0), 1, and 2 days postnatal mice were anesthesized with ether and perfused with Karnovsky's fixative for aqueous processing, or ethylene glycol for anhydrous processing. Mice were sacrificed and mandibular first molars were dissected. For culture of tooth organ, mandibular first molar tooth organs were dissected from timed-pregnant Swiss-Webster mice (Simonsen Labs, Gilroy, Calif., USA). We cultured E15 cap stage tooth organs for 11 and 18 days as previously described (Yamada et al. 1980; Bringas et al. 1987; Evans et al. 1988) and used BGJb medium (Fitton-Jackson's modified BGJ, GIBCO, Staten Island, N.Y., USA) supplemented with 100 μg/ml L-ascorbic acid and 100 U/ml penicillin/streptomycin. Explanted molars were cultured at 37.5°C with atmospheric conditions of 95% air and 5% CO_2. Initial pH was adjusted to 7.4 and the medium was changed every other day. All experiments were done in triplicate.

Histochemistry (von Kossa staining)

In vivo 0–2 day postnatal molar tooth organs were dissected, fixed in 10% buffered formaldehyde overnight and processed for embedding in Historesin^R. Sections were cut at a thickness of 1 μm and stained with von Kossa's technique for inorganic phosphates (Thompson and Hunt 1966).

Transmission electron microscopy of developing molar organs

In vivo postnatal molar tooth organs and E15 mandibular first molar explants cultured for 11 days in vitro in serumless medium, were sampled. Specimens were either fixed in Karnovsky's fixative for further transmission electron microscopy as previously described (Bringas et al. 1987; Evans et al. 1988), or were processed using an anhydrous preparation method (Landis and Glimcher 1982) to investigate initial crystal formation using electron-microprobe analysis. Sections were cut on a Reichert-Jung ultramicrotome. Thickness of sections was determined by comparing the interference colors of sections with a standard table. Sections were always cut from the enamel toward the dentine to avoid dislocations of enamel crystals away from the mineralized dentine. Ultrathin sections from Karnovsky-fixed tissues were contrasted in 1% uranyl acetate followed by Reynold's lead citrate for 15 min each. Sections from anhydrously processed tissues were post-contrasted in an alcoholic solution of 1% uranyl acetate no longer than 5 min. Observations were made on a JEOL 1200EX at 80 kV.

Sampling

After polymerization, Epon blocks were trimmed and re-embedded to provide sampling in which the mesiobuccal cusp of the mandibular first molar was always oriented perpendicular to the

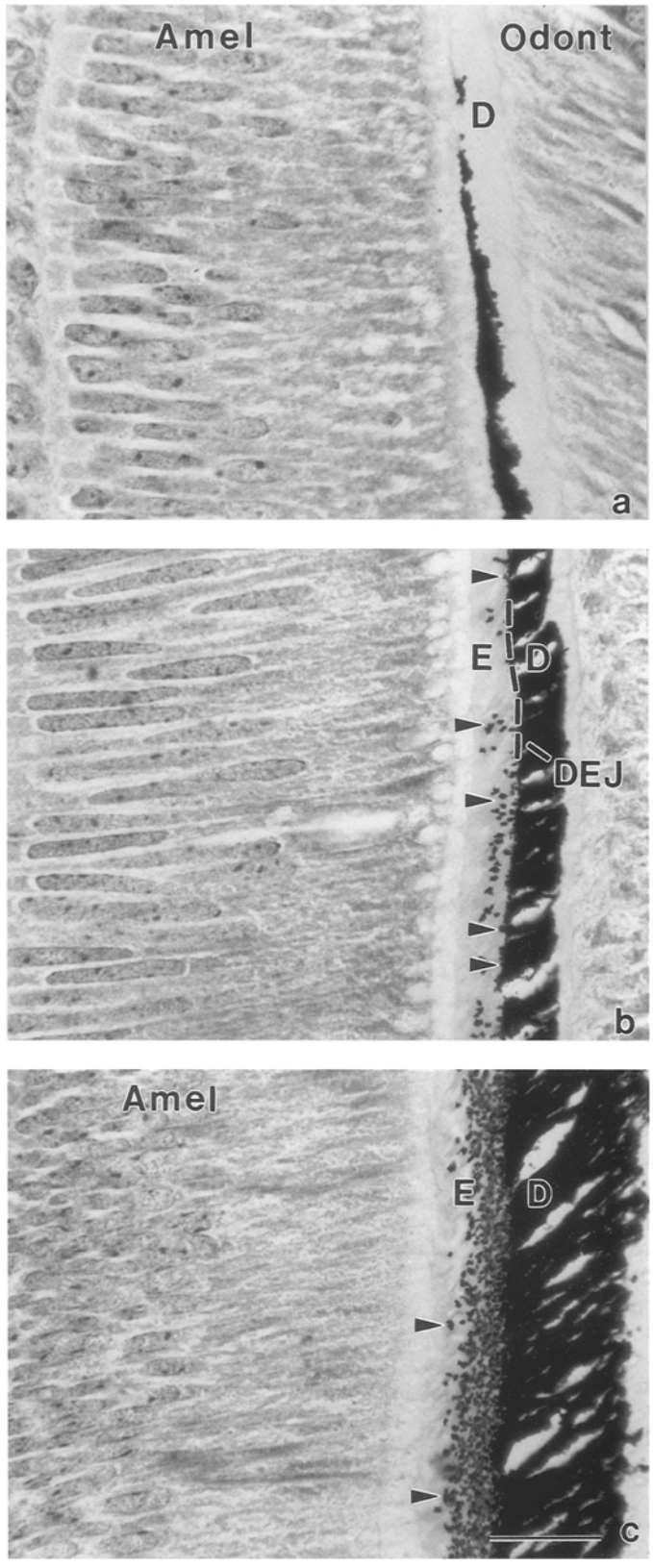

Fig. 1a–c. Developmental stages of dentine-enamel junction (*DEJ*) formation. Thick sections (1 μm) of Historesin^R-embedded material from 2 days postnatal molar development demonstrate calcium phosphate precipitates with von Kossa's stain. **a** Odontoblasts (*Odont*) have secreted mineralized matrix (dentine, *D*) parallel to proximal pole of ameloblasts (*Amel*). Unstained space is observed between ameloblasts and mineralizing dentine. **b** Enamel mineralized matrix has been secreted adjacent to previously formed dentine layer. Spheroid precipitates formed with von Kossa's procedure (*arrowheads*) are localized along dentine-enamel junction (DEJ). **c** Both dentine (*D*) and enamel (*E*) layers have increased in thickness. Enamel matrix is covered with intensely stained von Kossa-positive spherical granules (*arrowheads*). ×1 600. *Bar*: 10 μm

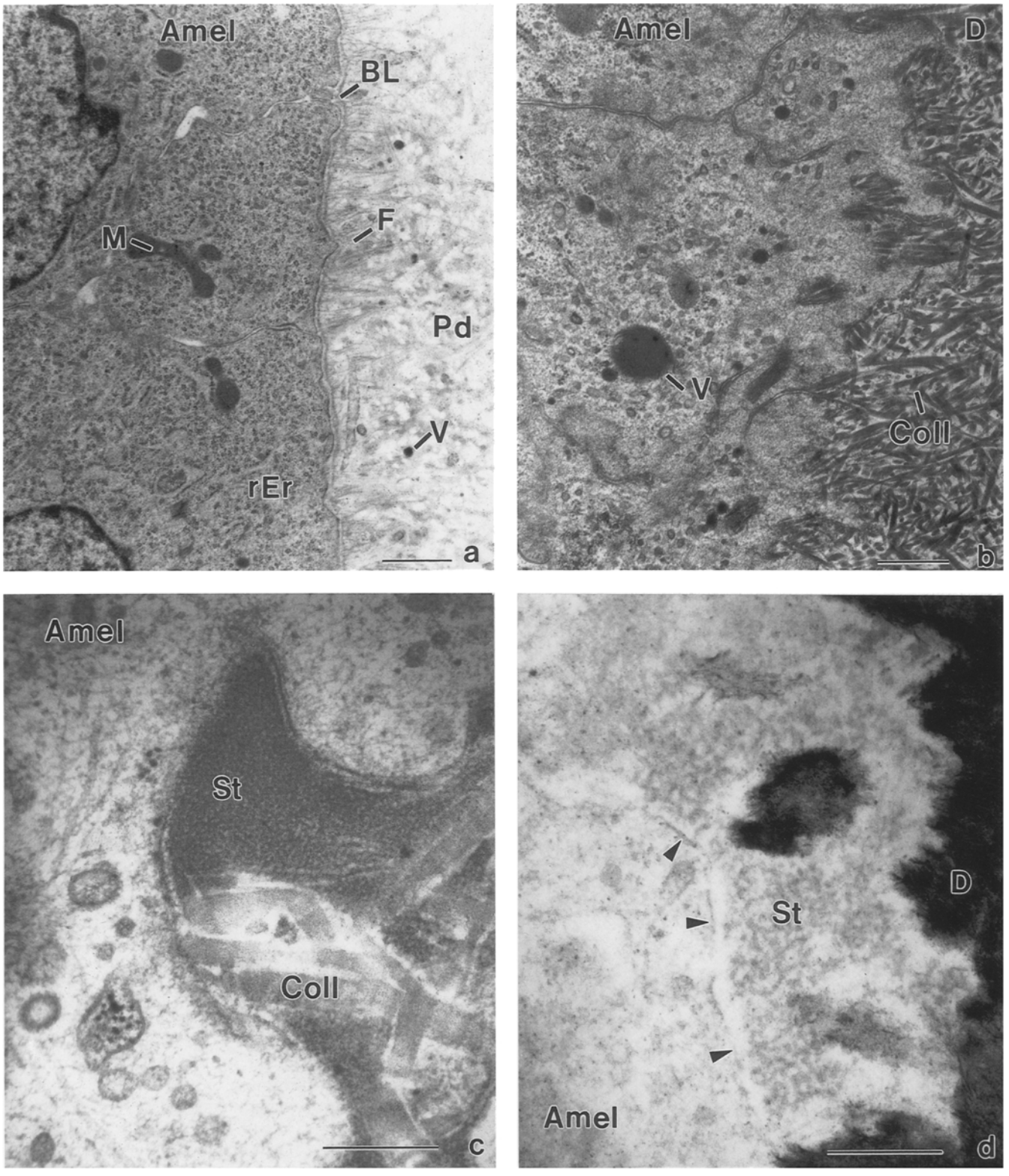

Fig. 2a–d. Sequential changes in the interface between ameloblasts and predentine prior to initial formation of enamel mineral. **a** Ameloblasts (*Amel*) and predentine (*Pd*) are separated by basal lamina (*BL*). Matrix vesicles (*V*) and filaments (*F*) are located in predentine adjacent to basal lamina. Mitochondria (*M*) and rough endoplasmic reticulum (*rER*) are present in proximal pole of ameloblasts. **b** Basal lamina is no longer detected along interface between ameloblasts (*Amel*) and predentine. Electron-dense spheres and vesicle-like structures (*V*) have accumulated at proximal pole of ameloblasts. Network of collagen fibers (*Coll*) is predominant in predentine. **c** Ameloblasts (*Amel*) have secreted stippled electron-dense materials (*St*) along interface with predentine. Thick collagen fibers (*Coll*) are visualized in close contact with electron-dense, stippled material (*St*). **d** Stippled material (*St*) has accumulated at interface between ameloblasts (*Amel*) and mineralized dentine (*D*) prior to initial enamel crystal formation. *Arrowheads* indicate cell membrane of ameloblasts. (**a**) ×12 000. *Bar*: 1 μm; (**b**) ×25 000. *Bar*: 500 nm; (**c**) ×50 000. *Bar*: 500 nm; (**d**) ×100 000. *Bar*: 200 nm

block-axis. Only the middle vertical plane was used for thin sectioning to ensure comparable sampling areas.

Electron-microprobe analysis

Specimens representing E15 mandibular first molars cultured for 11 days and developmentally comparable neonatal in vivo controls were isolated, fixed in ethylene glycol, and processed for either electron-microprobe or electron-diffraction analyses using the anhydrous preparation method (Landis and Glimcher 1982). Prepared samples were analyzed for Ca/P ratios in 5 independent regions of the forming enamel and dentine ECM by electron-diffraction microprobe analysis, using a Cambridge 360 scanning electron-microscope and LINK AN 10 000 EDS analyzing unit.

Crystal measurements

Ultrathin sections from 10 blocks per experimental group were analyzed to ensure random sampling. We used 10 electron-photomicrographs of randomly selected areas of each block near the forming dentine-enamel junction for further measurements. Crystal length measurements of 20 randomly selected crystals (crystal c-axis as revealed on micrograph) were taken (i) at the site of beginning crystal formation and (ii) in areas where the enamel width was 2 µm thickness. Measurements represented the average crystal length in c-axis direction as cut in 60 nm sections (gray-silver coloring using the Reichert-Jung ultramicrotome) and analyzed with 80 kV electron microscopy and not necessarily the entire crystal length. We determined the average crystal length per section and standard deviation.

Statistical analysis

Enamel HAP crystal length data was compared between enamel layers of 2 µm thickness formed in vitro with that formed in vivo. Ca/P ratios for both 11 and 18 culture days in vitro and postnatal days 2 and 7 in vivo were compared between enamel and dentine. Results were analysed using Student's *t*-test with a statistical software program (Instat^R). If both groups had significantly different standard deviations, an unpaired nonparametric test (Mann-Whitney2 sample test) was applied.

Electron microscopy of thick sections

To analyse anhydrously prepared sections of 1 µm thickness, we used the high voltage electron microscope Kratos EM 1500 of the National Center for Electron Microscopy in Berkeley, Calif., at 1.5 million volts. Sections were tilted in steps of 5° in each direction in x and y axis up to 20°. Within the resolution of the instrument, beam damage could not be reported after 2 h of operation.

Sections of 120 nm (gold coloring on Reichert-Jung ultramicrotome) of anhydrous preparations were analyzed using a JEOL 1200EX at 80 kV. Sections were tilted in x-axis up to 30° in steps of 5° in + and – direction.

Serial sections and 3D visualization of enamel crystals

Serial sections of Karnovsky-fixed 2 days postnatal mouse molars embedded into Epon were cut at 60 nm thickness (gray-silver coloring using Reichert-Jung ultramicrotome) and retrieved with uncoated 200 mesh copper grids.

Electron micrographs were taken at 50 000× magnification, printed on 8×10 inch high contrast paper and imported into an image analysis system using a tracing routine. A novel image analysis software was designed and programmed specifically to produce 3D reconstructions. Single images were aligned using a semi-automated routine.

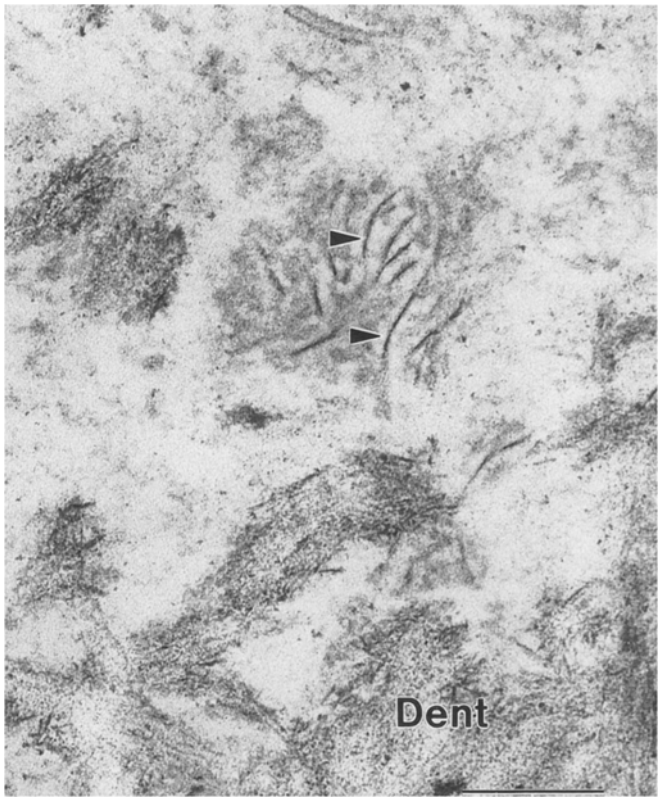

Fig. 3. Initial enamel crystals are not continous with mineralized dentine crystals. Short, randomly oriented initial enamel crystals (*arrowheads*) are embedded in electron-dense stippled material independent of mineralized dentine (*Dent*). × 180 000. *Bar*: 100 nm

Results

Initial biomineralization defines the dentine-enamel junction

The onset of biomineralization in the developing mouse molar was identified as a discrete interface along the future dentine-enamel junction (DEJ) using von Kossa's stain for anionic phosphate salts indicative of mineralization (Fig. 1). Initial mineral precipitates were formed in the mantle dentine in juxtaposition to the ameloblast layer (Fig. 1a). The mineralized mantle dentine increased in thickness relative to the predentine layer (Fig. 1a, b). Subsequently, unmineralized enamel matrix (*arrows*) was deposited against the mineralizing outer mantle dentine surface (Fig. 1b). Initial enamel matrix was characterized by only a few von Kossa-positive deposits (Fig. 1b), whereas the number of discrete spherical precipitates increased during further enamel maturation (Fig. 1c). Initial areas of mineralizing enamel were localized within the enamel matrix adjacent to the mineralizing dentine, defining the interface for the DEJ (Fig.

Table 1. Enamel crystal length per section

	Initial crystals	Crystals in enamel layers of 2 μm thickness	Significance (initial vs. 2 μm)
In vitro (E15+11d culture)	28.02 nm±15.16 nm S.D.	193.13 nm±123.78 nm S.D.	$P<0.01$
In vivo (2d postnatal)	49.27 nm±42.84 nm S.D.	314.29 nm±151.90 nm S.D.	$P<0.001$

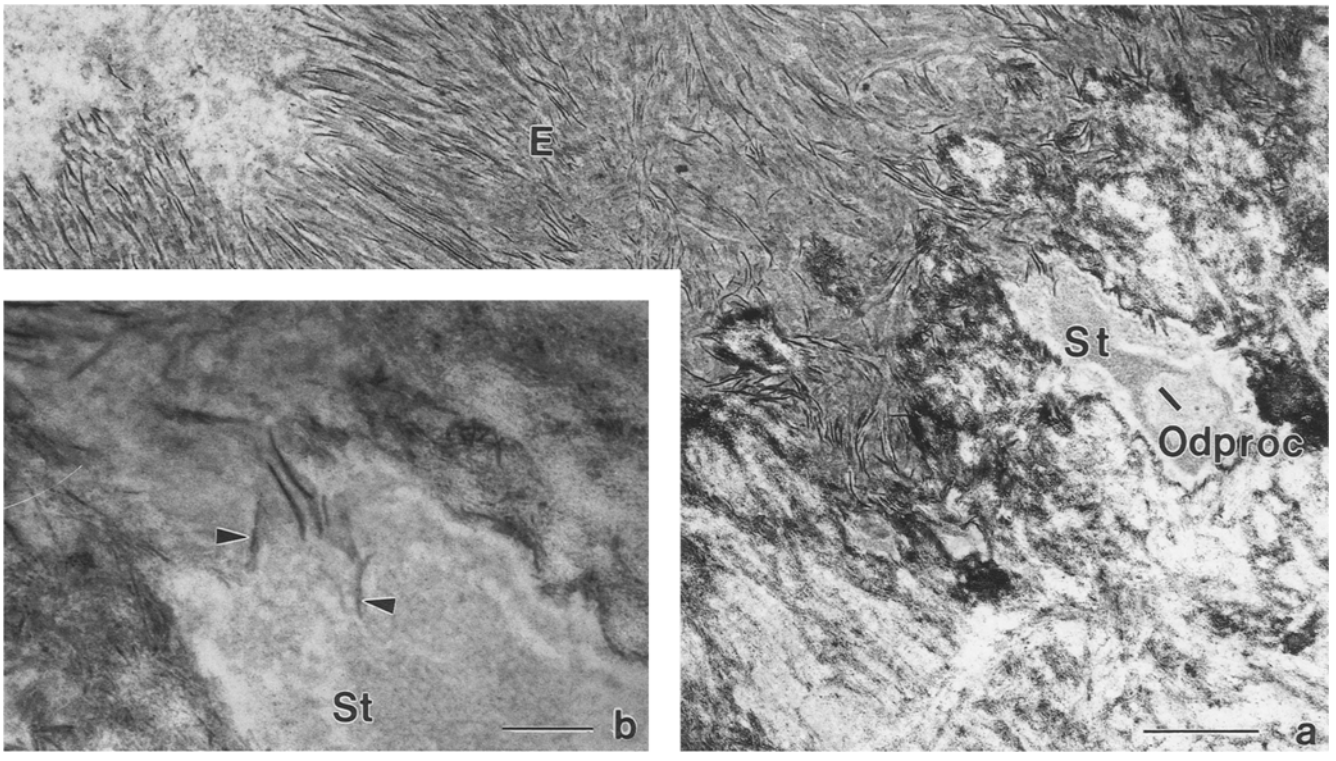

Fig. 4. **a** Odontoblast processes (*Odproc*) extend to mineralized enamel layer (*E*). Odontoblast processes are associated with electron-dense stippled materials (*St*) similar to stippled materials in enamel. **b** High magnification of **a**. Enamel crystals (*arrowheads*) near DEJ are associated with electron-dense stippled materials (*St*) positioned separate from adjacent dentine mineralized matrix. (**a**) ×30 000. *Bar*: 500 nm; (**b**) ×120 000. *Bar*: 100 nm

1b). A continuous progression of ameloblast differentiation and increased mineral deposition progressed along the DEJ from the apical to coronal aspects of the forming mandibular first molar mesiobuccal cusp region (Fig. 1b, c).

During mouse molar tooth development, the interface between ameloblasts and unmineralized dentine is defined by the basal lamina of the ameloblasts in Kallenbach differentiation zone III (Kallenbach 1971), (Fig. 2a). Microfilaments associated with the undersurface of the basal lamina and matrix vesicles define the DEJ in close proximity to the basal lamina (Fig. 2a). Subsequently, in Kallenbach differentiation zone V, the basal lamina was no longer present (Fig. 2b). Electron-dense, intracellular vesicles accumulated in the proximal pole of the ameloblast (Fig. 2b). At this stage, the predentine consisted of a network of thick collagen fibers (Fig. 2b). Within a space in juxtaposition to forming dentine matrix, ameloblasts secreted a characteristic extracellular matrix that consisted of electron-dense, stippled materials (Fig. 2c, d). Observations from a more coronal position included discrete and single enamel crystals or bundles of enamel crystals localized in aggregates of enamel stippled materials (Fig. 3).

Early enamel crystals formed at the DEJ were surrounded by stippled materials and different from mature enamel crystals

Enamel crystal orientation and extension changed during enamel formation, from short randomly oriented crystals at the initiation of enamel formation to long and oriented crystals within enamel layers thicker than 2 μm. The smallest clusters of crystals, localized to the apical region of the forming enamel layer, were embedded in matrices of electron-dense stippled materials of 200 nm thickness (Fig. 3) embedded in stippled materials. Initial crystals had an average length per section of 49.3 nm (±42.9 nm S.D.) and were not oriented (Table 1); these

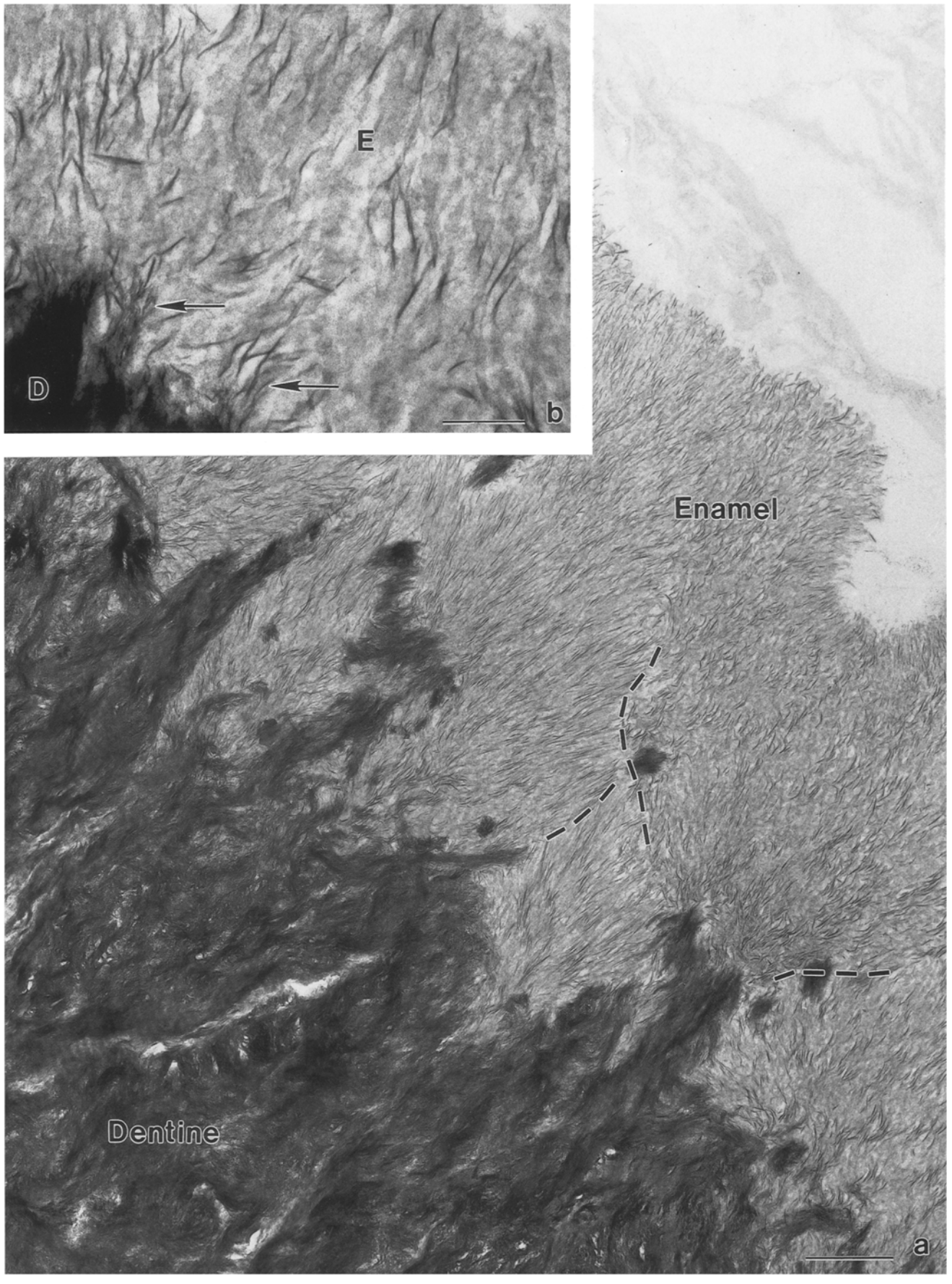

Fig. 5a, b. Anhydrous preparation of enamel mineralized matrix in 1 day postnatal mouse mandibular first molar. **a** Prisms of short and partially oriented enamel crystals originate from prominent points in dentine matrix. *Dashed lines* indicate outlines of adjacent enamel prisms. **b** High magnification shows relationship between growing enamel (*E*) crystals (*arrows*) and adjacent mineralized dentine (*D*). (**a**) ×80 000. *Bar*: 200 nm; (**b**) ×300 000. *Bar*: 50 nm

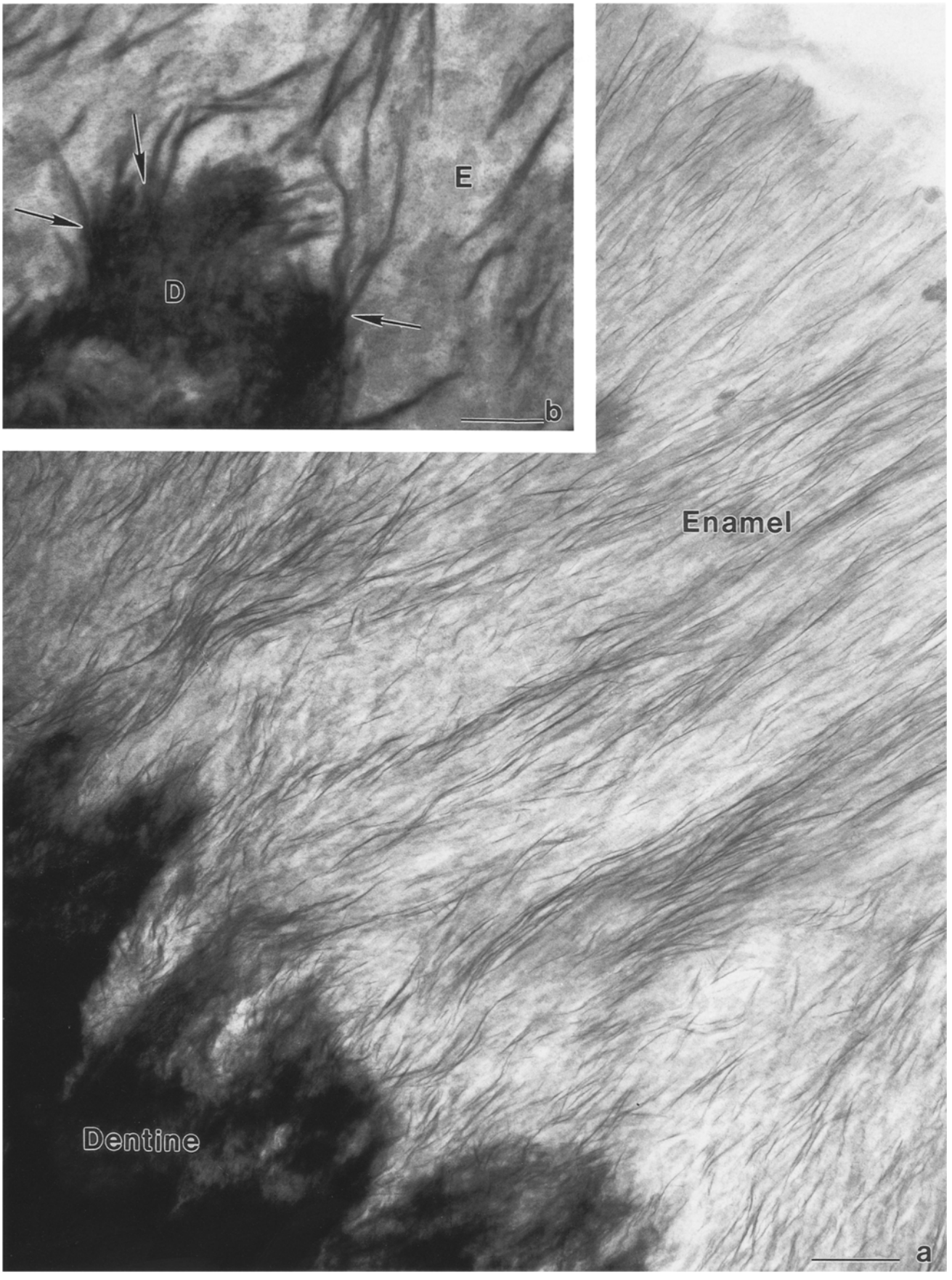

Fig. 6a, b. Anhydrous preparation showing mineralized matrix of enamel in a 2 days postnatal mouse mandibular first molar. **a** Long and parallel enamel crystals extend over entire enamel layer from DEJ to proximal pole of ameloblast. **b** Close to DEJ, enamel crystals are shorter and less oriented. The 120 nm thick section used for this anhydrous preparation did not allow electron-optical separation of enamel (*E*) and dentine (*D*) crystals (*arrows*). (**a**) ×80 000. *Bar*: 200 nm; (**b**) ×300 000. *Bar*: 50 nm

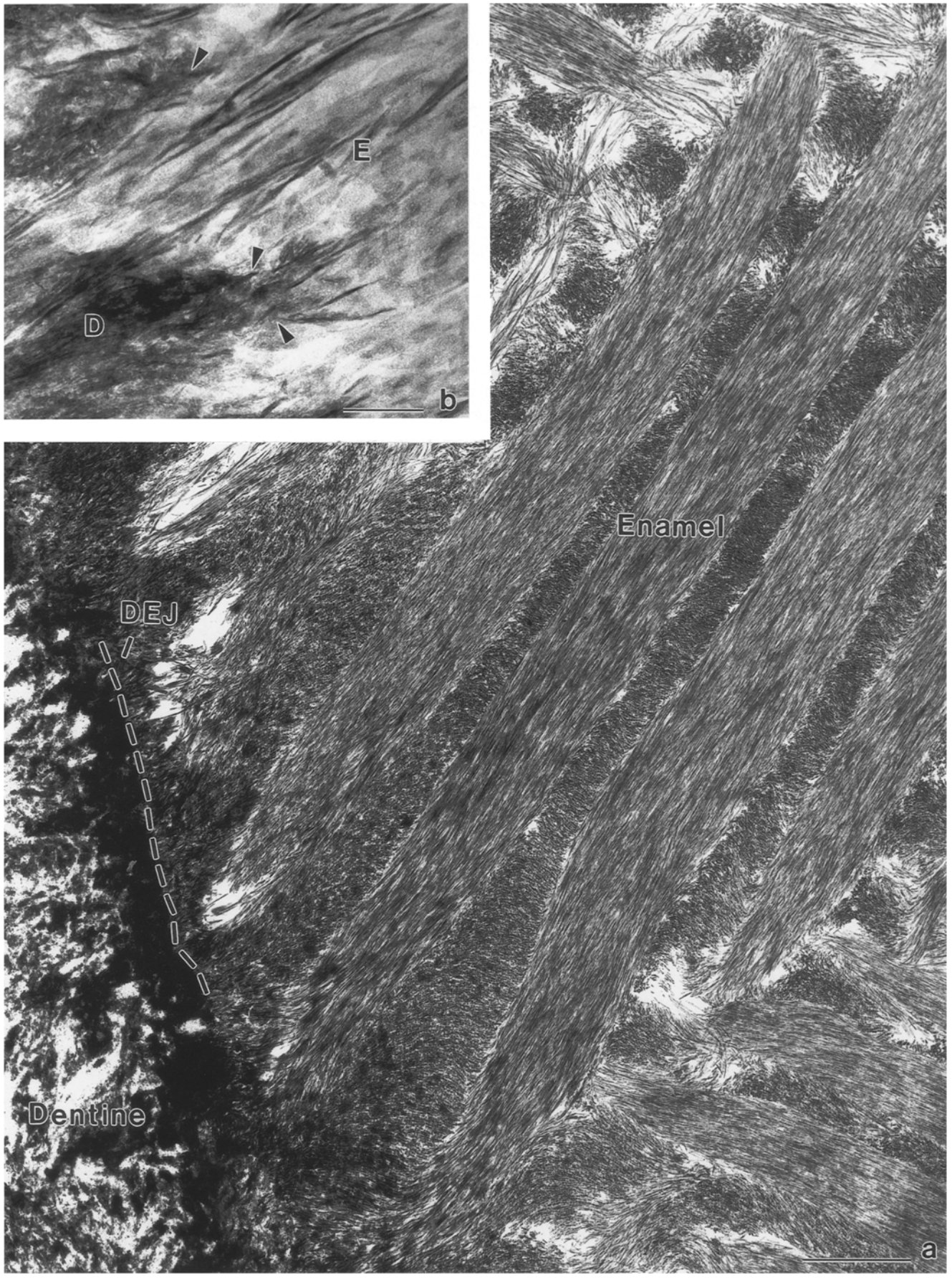

Fig. 7a, b. Enamel mineralized matrix of 7 days postnatal mouse mandibular first molar fixed in Karnovsky's fixative. **a** Enamel crystals are oriented in rods of long and parallel crystals originating from *DEJ* (*dashed line*). Alternating layers of rods are oriented 90° toward each other. **b** Enamel crystals (*E*) in proximity with dentine (*D*) mineralized matrix (*arrowheads*). (**a**) ×10 000. *Bar*: 2 μm; (**b**) ×300 000. *Bar*: 50 nm

Table 2. Calcium/Phosphorus (Ca/P) mass ratios in areas of developing mouse molar enamel

	Dentine (mean, S.D.)	Enamel (mean, S.D.)	Significance (enamel vs. dentine)
E15+11 days culture in vitro	1.31±0.18	1.26±0.13	Not significant
E15+18 days culture in vitro	1.81±0.12	1.95±0.09	$P<0.01$
2 days in vivo	1.72±0.13	1.53±0.12	$P<0.05$
7 days in vivo	2.12±0.07	2.31±0.05	$P<0.001$

crystals pointed in several directions and were arranged in varying angles toward each other. These relatively short crystals were separated from each other and from the adjacent dentine matrix by electron-dense stippled materials (Figs. 3, 8a, d, e). Enamel crystals, not connected to dentine crystals, were also localized to the surfaces of extended odontoblast processes (Fig. 4 a, b). These crystals were localized in the stippled materials associated with odontoblast processes (Fig. 4b).

During subsequent stages of mouse molar development, enamel crystals become continous with the DEJ

Enamel crystals increased in length and orientation as the enamel matrix increased in thickness (Table 1). In enamel layers of increasing maturation, crystals were oriented in bundles, but not parallel, and measured only a small percentage of the entire enamel thickness (Fig. 5a, Table 1). At this stage, a close relationship between enamel crystals and adjacent dentine mineralized matrix could be observed (Fig. 5b). However, we were not able to determine whether there was any direct continuity between enamel and dentine crystals. (Fig. 5b). Subsequent stages of maturing enamel contained long crystals which were parallel, highly oriented, and which seemed to be connected with the discrete DEJ (Figs. 6a,b, Table 1). Crystals in the enamel layer of 7 days old molars were even longer and more oriented (Fig. 7a). Rod- and interrod enamel alternated regularly, and alternating layers of rods were oriented at an angle of 90° toward each other (Fig. 7a). High magnifications of the DEJ revealed an intimate relationship between enamel crystals and mineralized dentine (Fig. 7b).

ACP, OCP and TCP represent the calcium phosphate phases of initial enamel crystals

Ca/P ratios of initially formed enamel matrix formed by E15 tooth explants cultured for 11 days in serumless medium were 1.26±0.13 S.D., whereas Ca/P ratios from comparably staged in vivo samples were 1.53±0.12 S.D.. These values were comparable to amorphous calciumphosphate (ACP) with a Ca/P ratio of 1.2 to 1.5 (Eanes 1973), octacalciumphosphate (OCP) with a Ca/P ratio of 1.33, and tricalciumphosphate (TCP) with a Ca/P ratio of 1.50, but not to HAP which requires a Ca/P ratio of 1.67 (Nancollas 1979, 1989) (Table 2). In 7 days postnatal molars, Ca/P ratios increased to 2.31±0.05 S.D. and exceeded the 1.67 required for HAP crystal formation (Table 2).

Tooth cultures in serumless, chemically-defined medium replicate the onset of enamel biomineralization and the sequence of dentine-enamel junction formation

The series of events during initial enamel biomineralization as reported were also replicated in our serumless organ culture model. Due to the characteristics of the culture system, which protracts events during mouse molar development, areas containing several stages of initial biomineralization were analyzed (Fig. 8a). Stages documented in this sampling area included (i) formation of the DEJ along long crystals representing the outer-most layer of dentine in juxtaposition to the ameloblast (Fig. 8b); (ii) secretion of electron-dense stippled material (Fig. 8c); (iii) formation of short and randomly oriented initial enamel crystals within the matrix of stippled materials, but not in contact with adjacent mineralized dentine (Fig. 8d); and (iv) enamel crystal orientation and elongation (Fig. 8e).

Clusters of enamel crystallites embedded in stippled materials were located up to 1 µm distance from the DEJ in vitro. Initial crystals measured 28.02 nm (±15.16 nm S.D.) in average length per section and were surrounded by electron-dense stippled materials (Fig. 8d, e, and Fig. 9, D_6, D_7). No evidence for crystal continuity with the adjacent dentine was observed (Fig. 8d). Using the organ culture system, we analyzed the distribution of the electron-dense material at the interface between stippled materials containing no crystals and adjacent areas of initial enamel crystal formation. The stippled material was compartmentalized into subunits (Fig. 9a). The distance between adjacent electron-dense subunits as well as the distance between adjacent negatively stained subunits was approximately 20 nm (Fig. 9, D_1, D_2), a value which was equivalent to the distance between two adjacent initial crystallites (Fig. 9, D_3). The characteristic organization of the organic matrix changed from the regular granular pattern in the stippled materials toward electron-dense coats surrounding the initial crystals (Fig. 9a, b). This electron-dense material surrounded the intial enamel crystallites with a coat measuring between 3 and 10 nm in diameter while the initial crystal measured only between 1 and 3 nm in diameter (Fig. 9b, D_4, D_5). In our culture system we observed a comparable increase in size of enamel crystals as documented in vivo; in enamel layers measuring 2 µm thickness or more, crystals mea-

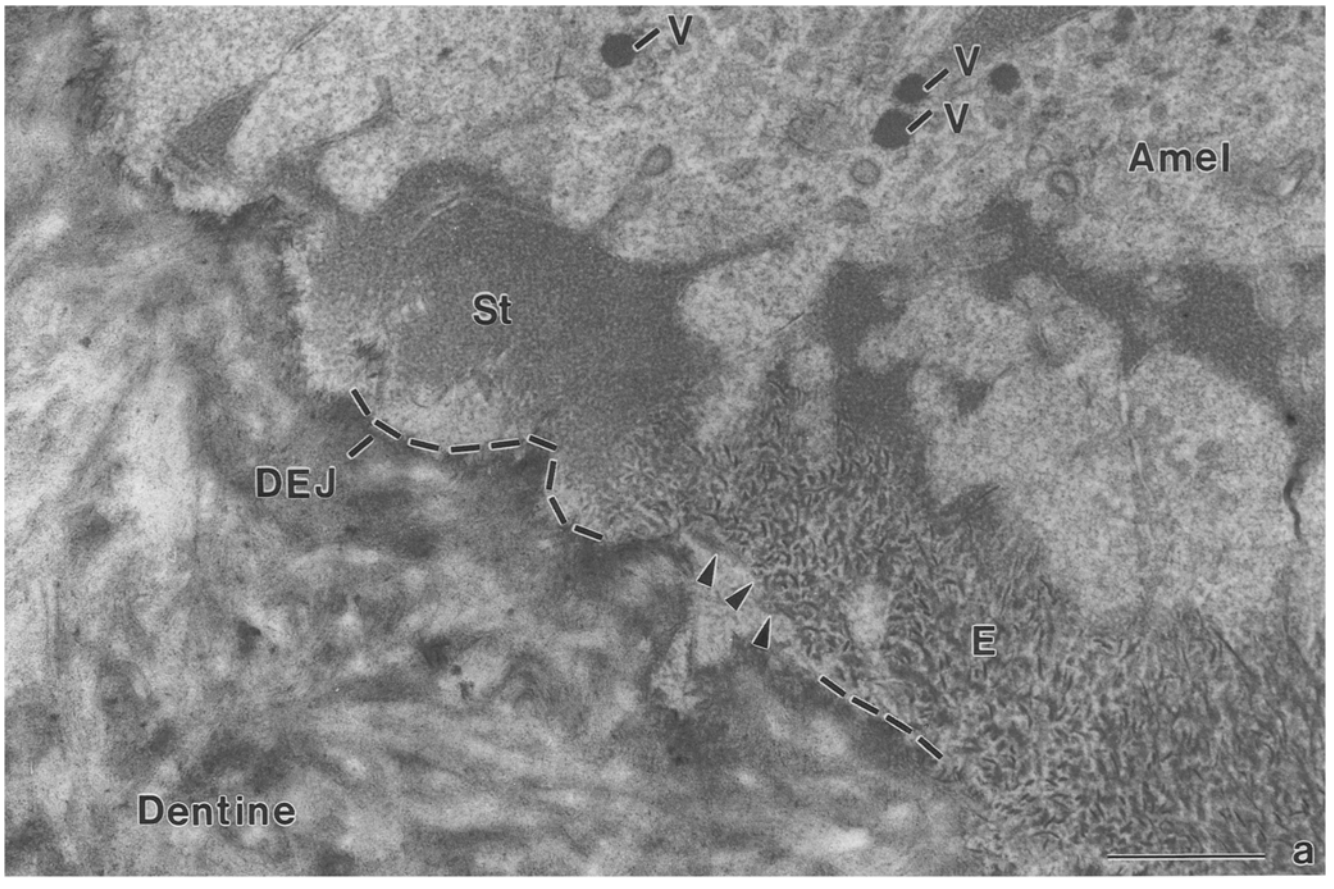
V
V
V
Amel
St
DEJ
E
Dentine
a

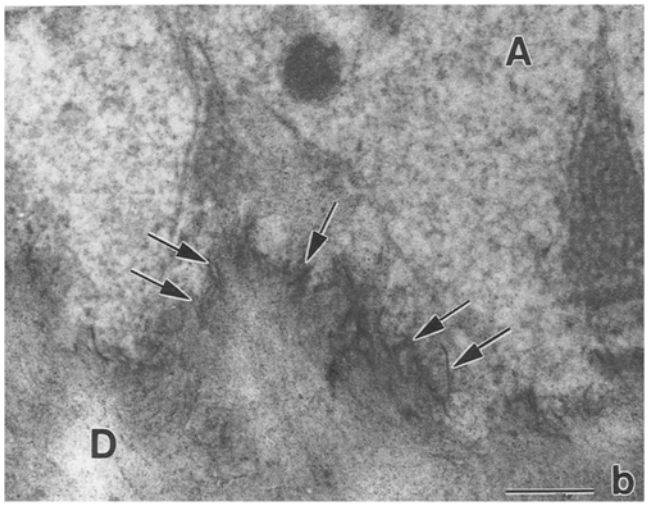
A
D
b

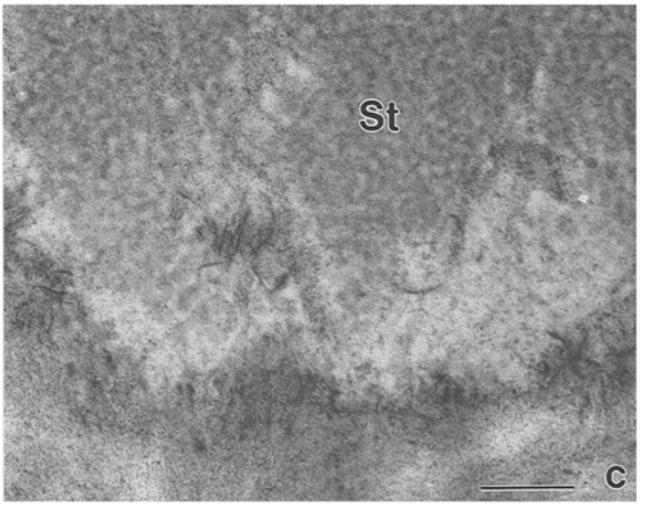
St
c

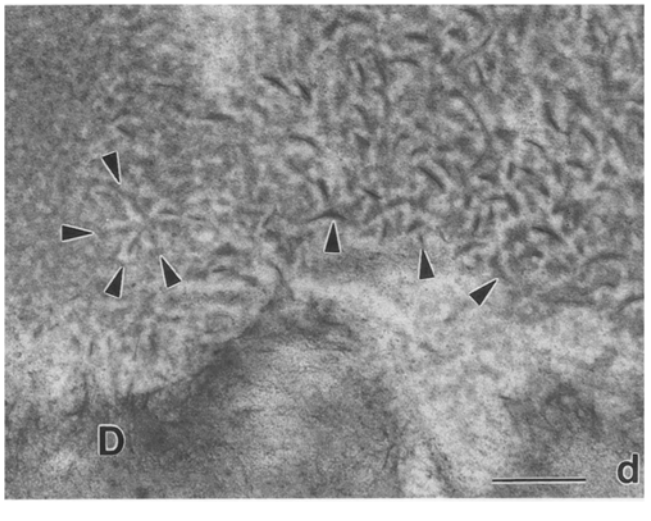
D
d

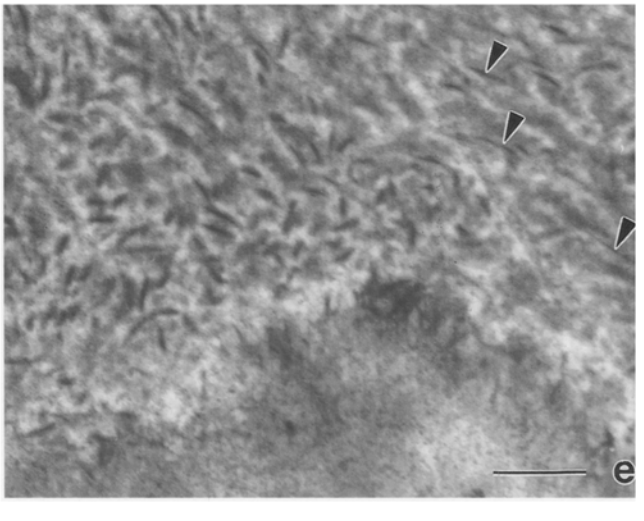
e

sured 193 nm (±123 nm S.D.) in average length per section (Table 1).

Ca/P ratios indicated that E15 embryonic mouse mandibular molar organs cultured in serumless, chemically-defined medium expressed normal patterns of initial tooth enamel biomineralization. Microprobe analyses of Ca/P ratios of enamel and dentine biomineralization within cultured tooth explants at 11 and 18 days in vitro were comparable to measurements of 2 and 7 days postnatal molar tooth enamel and dentine as shown in Table 2. Ca/P mass ratio values for cultured molars and in vivo samples exceeded unity in dentine as well as in enamel; a value established as indicative of mineralization (Lee et al. 1986; Landis and Glimcher 1982). In general, values for the in vivo samples were slightly higher than for the in vitro samples.

Initial individual enamel crystals and early clusters of enamel crystals do not extend from the mineralized dentine

In our investigations of the spatial relationship of clusters of early enamel crystals in juxtaposition to forming adjacent dentine matrix, we observed discrete enamel crystals not connected to the mineralized dentine matrix.

Thick (120 nm gold color using the Reichert-Jung ultramicrotome) sections of anhydrously prepared tissues were observed using the tilting routine of the medium voltage transmission electron microscope. We identified clusters of enamel crystals not connected to the matrix of dentine crystals (Fig. 10).

Using high voltage transmission electron microscopy, a cluster of early enamel crystals was identified containing several isolated crystals not connected to the dentine matrix. The section of 1 μm thickness was tilted in the x-axis while the cluster of crystals was placed in the center of the electron beam (Fig. 11). Analysis of the pictures revealed isolated crystals not connected to the dentine matrix. In some instances where crystals appeared to be connected, tilting of the section demonstrated that this effect was caused by superimposition (Fig. 11G).

Serial sections were cut and analyzed to reveal length, extension, and orientation of crystals in areas as thick as 300 nm, representing 5 serial sections of 60 nm thickness (silver-gray color using a Reichert-Jung ultramicrotome). These sections were thin enough to obtain a 50 000× image of the section in its entire thickness so that the electron beam would project each crystal within the section. Crystals did not continue over more than 2 sections, but were essentially restricted to single section. We identified both single and clusters of enamel crystals which did not connect to the mineral constituents of the dentine matrix (Fig. 12, arrows).

Discussion

The present study provides the first evidence that initial enamel crystal nucleation and growth are spatially independent from dentine crystal formation. Discrete individual enamel crystals were localized separate from the dentine mineralized matrix along the forming DEJ. Based on these observations we suggest a sequence of 3 major processes that control initial enamel formation: (i) establishment of a suitable microenvironment associated with the removal of the basal lamina and the secretion of electron-dense, stippled material; (ii) initial calcium phosphate crystal formation within aggregates of electron-dense, stippled material separate from the dentine matrix; and (iii) formation of long enamel HAP crystals which eventually extend to the dentine mineral. The following discussion focuses on possible mechanisms of enamel formation, the growth, and maturation of enamel crystals during development, and the significant role of the organic matrix surrounding initial enamel crystals.

Mineralization of all vertebrate calcifying tissues other than enamel involves the deposition of calcium phosphate and the formation of calcium hydroxyapatite in association with collagen. In the initial stages of dentine mineralization, matrix vesicles and type-I collagen provide a template for calcium hydroxyapatite mineral to deposit in an orderly fashion (Anderson 1973; Slavkin 1973; Wuthier 1992; Yamauchi et al. 1992). This interpretation has been supported by tomographic reconstructions from high voltage electron microscopy of newly mineralized turkey tendon that provided direct 3-dimen-

Fig. 8a–e. Organ culture-replicated sequence of early enamel biomineralization and dentine-enamel junction (*DEJ*) formation. **a** Developmental stages of biomineralization from upper left to lower right corner. Electron-dense stippled materials (*St*) of enamel are located between DEJ and ameloblasts (*Amel*). Intracellular secretory vesicles (*V*) are associated with electron-dense stippled material observed in forming enamel matrix. Within organic matrix, initial enamel crystals (*E*) have formed independent from DEJ (*arrowheads*) and are entirely surrounded by organic matrix. *Dashed lines* indicate DEJ interface. **b–e** Survey of stages of initial enamel biomineralization in organ culture. **b** Formation of DEJ along long crystals (*arrows*) representing outermost layer of dentine (*D*) facing ameloblasts (*A*). **c** Electron-dense stippled materials (*St*) as microenvironment for enamel crystal nucleation. **d** Short and randomly oriented enamel crystals (*arrowheads*) have formed within stippled material matrix but not in contact with adjacent mineralized dentine (*D*). **e** During enamel maturation, enamel crystals become longer and more oriented (*arrowheads*). (**a**) ×40 000. *Bar*: 500 nm; (**b–e**) ×120 000. *Bar*: 100 nm

Fig. 9a, b. Changes in organization of stippled material matrix related to initial formation of enamel crystal in mouse molar organ culture using serumless medium. **a** Characteristic organization of regular granular pattern in stippled material matrix (*St*) changes to electron-dense coats (*arrowheads*) along surface of initial crystals in proximity to secretory ameloblasts (*Amel*). Distance between subunits of stippled "beaded" material is relatively constant and comparable to distance between initially formed crystals: D_1 distance between 2 adjacent negatively stained subunits=20 nm; D_2 distance between 2 adjacent electron-dense subunits=20 nm; and D_3 distance between 2 adjacent initial crystallites=20 nm. **b** Electron-dense material coats initial enamel crystallites with electron-dense material measuring between 3 and 10 nm in diameter (D_4= 5 nm). Initial crystals measure between 1 and 3 nm in diameter (D_5=1.5 nm) and 15 to 50 nm in length (D_6=50 nm, D_7=25 nm). (**a**) ×250 000. *Bar*: 100 nm; (**b**) ×400 000. *Bar*: 25 nm

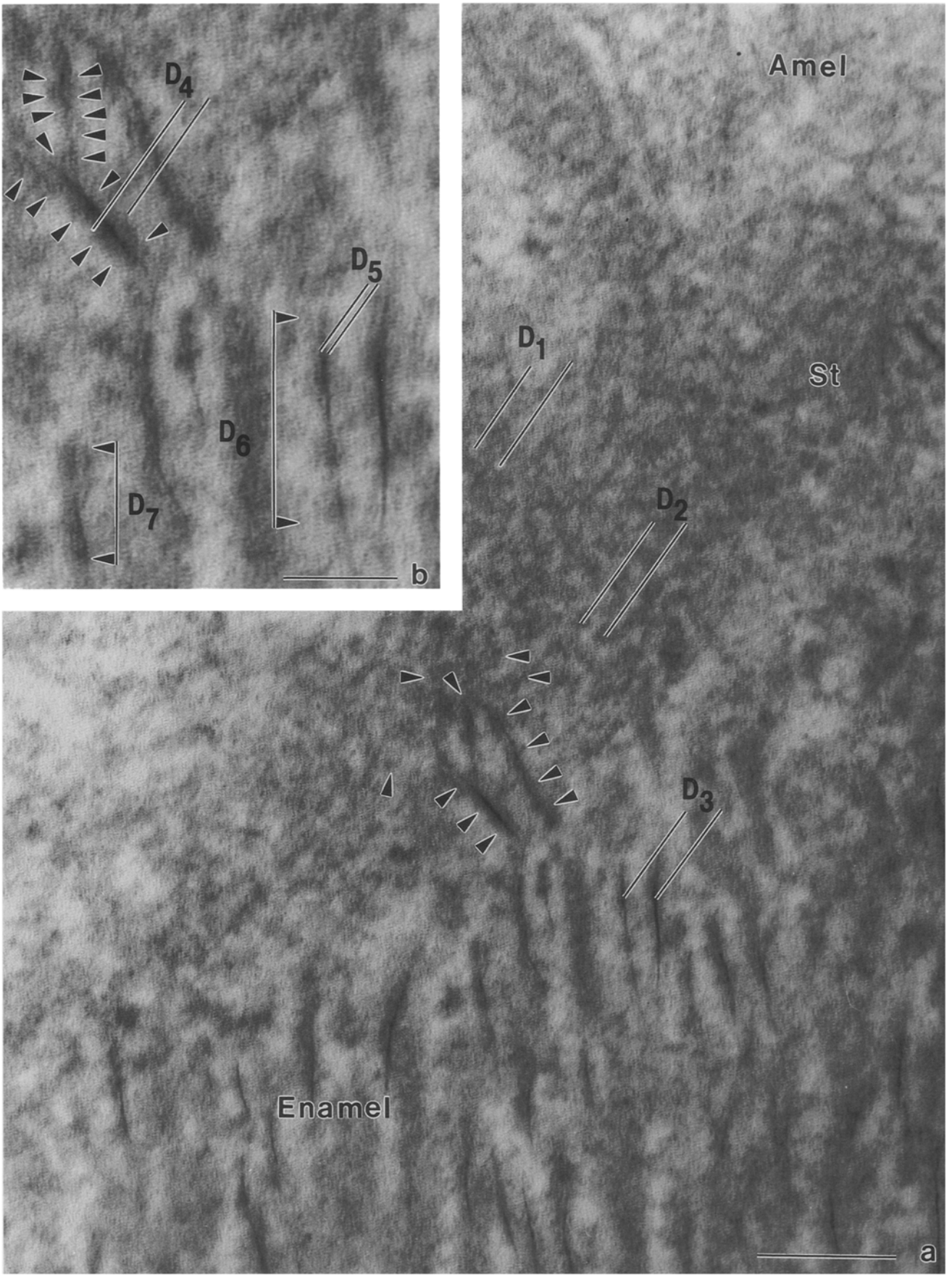

Fig. 9a, b.

Fig. 10a–g.

sional images. These images illustrated a possible spatial and temporal sequence by which mineral crystals associate with type-I collagen during normal calcification (Landis et al. 1992). Since matrix vesicles as well as collagen fibres are not present in forming enamel, nucleaton of enamel crystal is assumed to be controlled by the unique protein matrix consisting of amelogenins and enamelins (Robinson et al. 1982; Aoba et al. 1989; Fincham et al. 1991). While several authors have supported the concept of enamel crystal growth control by constituent proteins in the organic enamel matrix (Doi et al. 1984; Diekwisch et al. 1993), the mechanisms for nucleation of enamel crystal remain unclear.

In general, crystal formation requires a supersatured solution and a nucleating event. A solution is supersaturated when the ionic concentration exceeds its solubility product. Putative nucleating events for enamel crystallization include: (i) contact with dentine crystals (Lehner and Plenk 1932; Reith 1967; Bernard 1972; Fearnhead 1979; Arsenault and Robinson 1989); (ii) charged macromolecules (Höhling 1966) like enamelins; i.e. tuftelin (Deutsch 1989), collagen (Boyde 1964; Höhling et al. 1981; Arsenault and Robinson 1989; Landis 1985, 1986), serum proteins (Limeback 1991; Goodman et al. 1991; Infante and Gillespie 1977) or proteins of the basement membrane (Deutsch 1989; Fincham et al. 1992); and (iii) specific properties of amelogenins (Glimcher 1979). In our study, we report the nucleation of initial enamel crystals spatially independent of dentine crystals or dentine collagen. We document initial crystals embedded into an organic matrix of electron-dense stippled material, and suggest that initial crystal formation takes place within this microenvironment of electron-dense stippled materials (Figs. 3, 8, 9). Our study does not provide evidence as to the direct role of amelogenins, enamelins, or other proteins in enamel crystal nucleation or crystal growth (Aoba et al. 1989; Diekwisch 1993). However, our analysis of forming enamel in cultured molars (Figs. 8, 9) suggest parallels between the novo enamel crystal formation within or between enamel-specific protein aggregates and the formation of apatite crystals within or between the collagen fibers in developing bone (Landis 1985, 1986).

We concede that in some instances initial crystals might have been closely associated with mineralized matrix of the dentine, while adjacent crystals appeared not to be associated with the dentine (Fig. 10). However, the demonstration of clusters of initial crystals not associated with the adjacent dentine suggests other mechanisms for initial crystal nucleation of enamel besides originating from mineralized dentine. Although the present study provides ample evidence to support the hypothesis that initial enamel crystals are formed independent of the mineralized dentine, our observations cannot give a definitive answer to the question of the origin of the first enamel crystals, especially since ameloblasts and organic matrices are easily deformable during manipulations required for preparation, fixation, and embedding. Furthermore, biochemical or physical inductive effects of the adjacent dentine cannot be excluded.

We measured crystal length per section to document the relative increase in crystal size during enamel maturation (Table 1). Our data for the length per section of the most recently deposited enamel crystals at the DEJ (Table 1) were significantly smaller than the length data previously reported by Travis and Glimcher (1964; 130 nm length for most recently deposited enamel crystals); approximately 1/6 of the length of the crystals in layers of 2 μm thickness. Measurements of crystal length in ultrathin sections do not document the entire length of the crystals. However, in our study they indicate that initial crystals are relatively short, and that early crystals grow many times their initial length until they form mature enamel.

Initial enamel crystals were not only different from more mature enamel crystals in terms of crystal size and orientation, but they also were different in their Ca/P ratios (Table 2). Ca/P ratios of 1.26 (in vitro) and 1.53 (in vivo) in initially formed enamel layers were comparable to amorphous calcium phosphate (ACP) with Ca/P ratios between 1.2 and 1.5 , octacalciumphosphate (OCP) with a Ca/P ratio of 1.33, and tricalciumphosphate (TCP) with a Ca/P ratio of 1.50 (Nancollas 1979, 1989; Johnsson and Nancollas 1992). Our observations are in agreement with those reported by Landis and colleagues who found Ca/P ratios of 0.99–1.46 (average 1.24±0.15) in earliest apical enamel areas (Landis et al. 1988). The Ca/P mass ratios of enamel crystals later in development exceeded the 1.67 required for HAP crystal formation (Table 2) (Young 1973; Nancollas et al. 1979, 1989).

We interpret these data to support the concept that during initial enamel formation, short and unoriented crystals of a low calcium phosphate ratio are formed. Several authors have investigated the transformation of calcium phosphates of a low ratio into hydroxyapatites (Eanes 1973; Eanes et al. 1973; Heughebaert and Montel 1973; Johnsson and Nancollas 1992; Newesely 1973). We propose that in initial enamel, short and randomly oriented crystals are of a calcium phosphate phase with a lower Ca/P ratio than HAP, but since they are crystalline they contain TCP or OCP and not ACP. As Bonucci (1973) has suggested, only a few calcifying globules are required to initiate a process of matrix-mediated mineralization. Following this proposal, initial crystallites of low Ca/P ratios and adjacent mineralized matrix of the dentine may be required for the formation of long HAP crystals characteristic of enamel (Figs. 5–7).

We observed a change in the characteristic organization of the organic enamel matrix between those areas which did not contain crystals, and adjacent areas containing initial enamel crystallites (Figs. 4b, 8a, d, and 9). In areas containing no crystallites, electron-dense stip-

Fig. 10a–g. a Initial enamel crystals (*Enamel*) forming along dentine matrix (*Dentine*) in anhydrous preparation. Short, randomly oriented crystals (*arrowheads*) have been transformed into, or replaced by, longer organized crystals (*arrows*). **(b–g)** Series of tilted aspects of initial enamel crystals further to the left than **a**. Center was tilted 30° with 5° incident in 120 nm thick anhydrous preparation. Initial enamel crystals (*arrowheads*) are not associated with mineralized dentine (*D*) independent of angle of electron beam. **(a)** ×30 000. *Bar*: 500 nm; **(b–g)** ×75 000. *Bar*: 200 nm

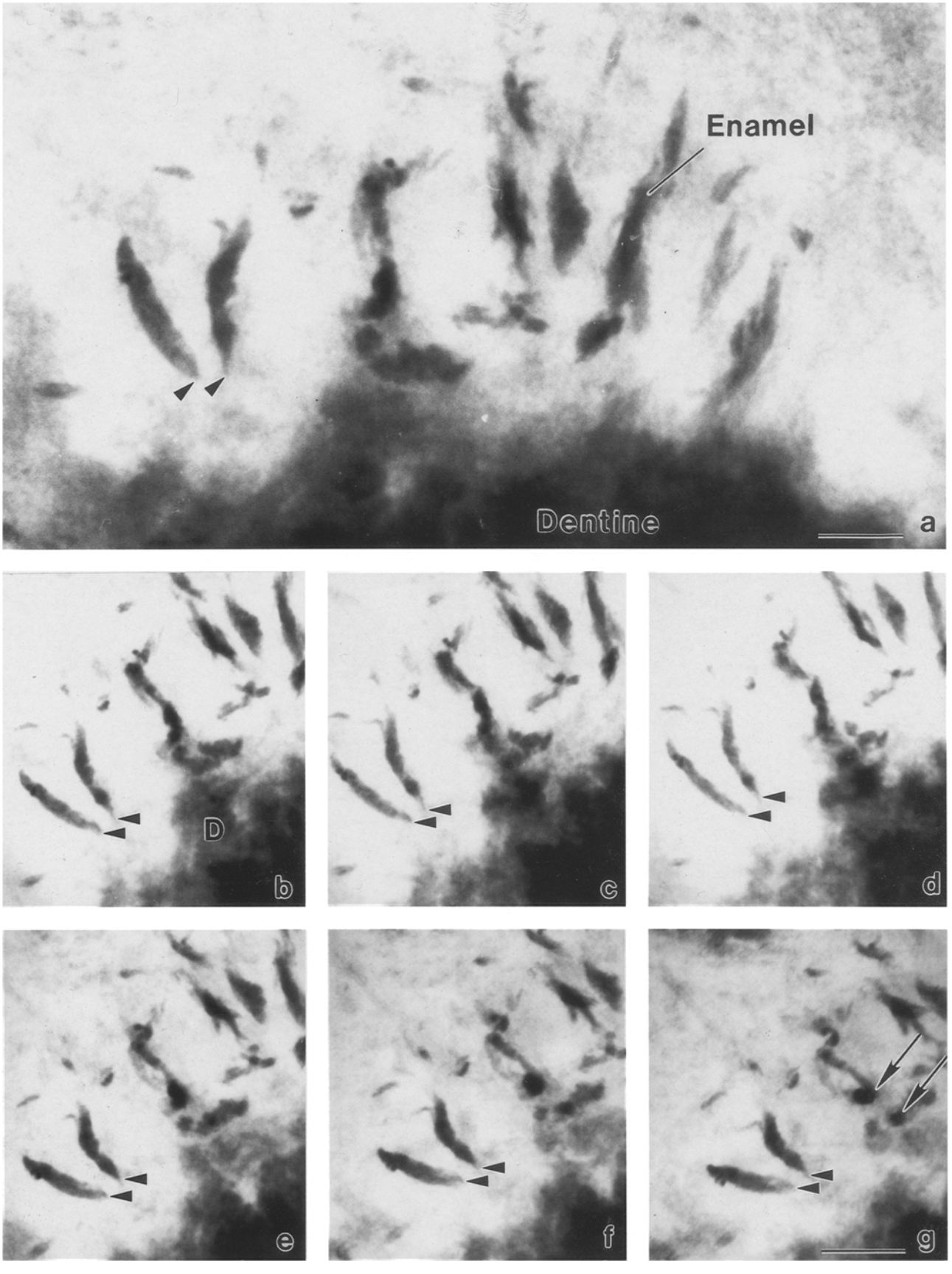

Fig. 11. a High 1 million voltage transmission electron photomicrographs of initial enamel crystals (*Enamel*) adjacent to mineralizing dentine (*Dentine*). 1-μm-thick section tilted in the x-axis direction from +5 ° to +15° (**b–d**), and from −5° to −15° (**e–g**). Group of enamel crystals at left (*arrowheads*) is not associated with mineralized dentine. These 2 *arrowheads* indicate identical crystals that remained in center of beam during tilting sequence. Group of enamel crystals at right (*arrows*) could be demonstrated to be separate from adjacent dentine after tilting by −15° (**g**). (**a**) ×30 000. *Bar*: 500 nm; (**b–g**) ×75 000. *Bar*: 200 nm

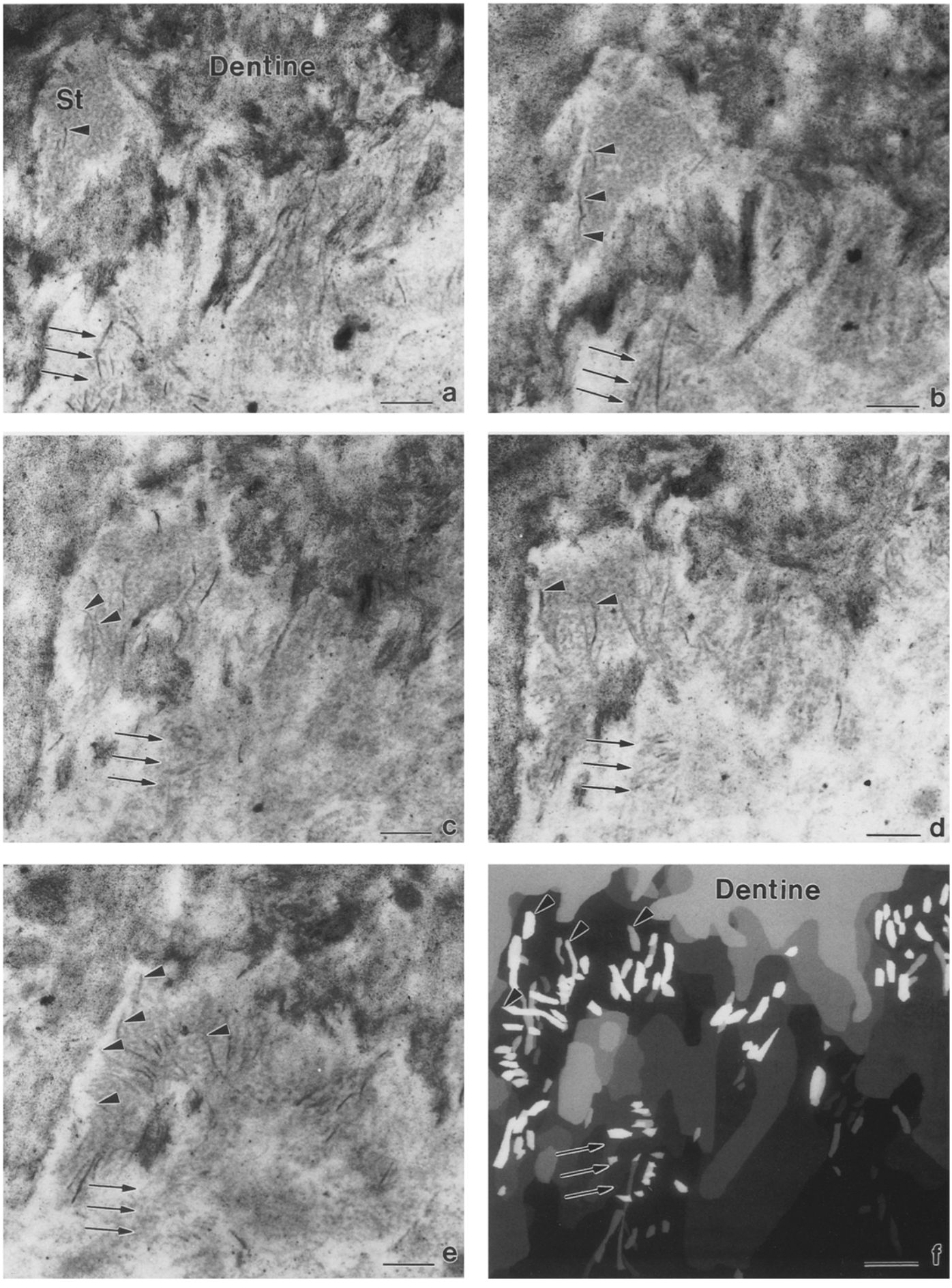
Dentine
St
a
b
c
d
e
Dentine
f

pled materials were organized in a random granular fashion (Figs. 8a, c, 9). In the interface between stippled materials and crystallites, the electron-dense organic matrix lost its granular pattern, and appeared to surround the initial enamel crystallites (Figs. 8a, d, e, 9b). Although there is no direct evidence proving that the organic matrix surrounding the initial crystals is identical to the organic matrix in the granules of the stippled materials, ultrastructural observations as shown in Figs. 8a, e, and 9 suggest that enamel protein aggregates in the stippled zones are continous with the electron-dense coats around initially formed crystals.

Several lines of evidence should be considered. First, Nanci et al. (1985) and Hayashi et al. (1986) have reported immunocytochemical studies in which this coating material around crystallites as well as the stippled material reacted with antibodies against amelogenin. Second, this electron-dense material surrounding the enamel crystallites is also observed in later stages of enamel development (Figs. 5–7b). Third, organic material surrounding enamel crystals has been described as crystal ghosts (Frank et al. 1960; Reith 1960; Bonucci 1979; Kallenbach 1982, 1986; Nanci et al. 1983; Warshawsky; 1989) and suggested to consist of organic matrix because of its close association with the forming enamel crystal (Bonucci 1984). The experiments of Slavkin et al. (1976) using autoradiography of ^{3}H tryptophan-labeled proteins provided direct evidence for the metamorphosis of enamel proteins from the stippled material to proteins of the forming enamel matrix. Finally, Travis and Glimcher (1964) suggested that this organic matrix is a template for the inorganic crystals, whereas other authors observed this material as fibrillar (Frank et al. 1960), lamellar (Roennholm 1962), or helical structures (Smales 1975), and to represent an organic mantle of the enamel crystals. We interpret the sudden change in the organic enamel matrix from granular stippled material toward electron-dense ghosts surrounding initial crystals as indicative of an involvement of the amelogenins in the growth of enamel crystals. This observation supports and explains previous hypotheses and experiments suggesting an involvement of amelogenins in the control of enamel crystal length and habit (Robinson et al. 1982; Aoba and Moreno 1989; Yanagisawa et al. 1989; Fincham et al. 1991; Diekwisch et al. 1993; Nelson and Barry 1989).

In summary, the present study provides evidence to support the hypothesis that de novo nucleation and growth of enamel HAP crystal are independent of the mineralization processes characterized for dentine. Our study further indicates that early enamel crystals are small and short crystals of TCP or OCP embedded in a matrix of organic stippled materials. In later stages of enamel formation, enamel crystals transform into long and parallel-orientedHAP crystals which could not be observed to be separate from dentine HAP crystals.

Fig. 12a–f. Serial sections of initial enamel crystals embedded in stippled materials (*St*) adjacent to mineralized dentine (*Dentine*). (**a–e**) Sequence of 5 consecutive sections, and (**f**) a 3-dimensional reconstruction based on 5 serial sections shown in **a–e**. Initial enamel crystals are not in contact with adjacent dentine mineral. Crystals identified by triplet of arrows or arrowheads do not continue from one section to another (*arrows, arrowheads*) indicating that they are so short and thin that their entire length is limited to one section; they did not extend to dentine mineral in an adjacent plane of section. White, less electron-dense space could be observed between initial enamel crystals and adjacent dentine. ×50 000. *Bar*: 200 nm

Acknowledgements. The authors would like to thank Douglas Owen and the National Center for Electron Microscopy in Berkeley, Calif., for the use of the high voltage electron-microscope. Thanks to Mr. Pablo Bringas Jr. for dissecting the cultured E 15 mouse molars and Mr. Valentino Santos for preparing specimens and staining using the von Kossa's procedure. These studies were supported in part by funds from the National Institute For Dental Research (NIDR), NIH, USPHS, grants DE-02848 and DE-06425 (H.C.S.). T.D. was supported by Postdoctoral Fellowship DFG grant Di 427/1–1.

References

Anderson HC (1973) Calcium-accumulating vesicles in the intercellular matrix of bone. Ciba Found Symp 11:213–246

Aoba T, Moreno EC (1989) Mechanism of amelogenetic mineralisation in minipig secretory enamel. In: Fearnhead RW (ed) Tooth Enamel V. Florence Publishers, Yokohama, pp 163–167

Aoba T, Moreno EC, Kresak M, Tanabe T (1989) Possible roles of partial sequences at N- and C-terminal of amelogenin in protein-enamel mineral interaction. J Dent Res 68:1331–1336

Arsenault L, Robinson BW (1989) The dentino-enamel junction: a structural and microanalytical study of early mineralization. Calcif Tiss Int 45:111–121

Bernard GW (1972) Ultrastructural observations of initial calcification in dentine and enamel. J Ultrastruct Res 17 41:1–17

Bonucci E (1973) The organic-inorganic relationships in calcified organic matrices. In: Physico-Chimie et Cristallographie des Apatites d'intérét biologique. Colloques internationaux du centre national de la recherche scientifique 230, Paris, pp 231–246

Bonucci E (1979) Presence of crystal ghosts in bone nodules. Calc Tiss Int 29:181–182

Bonucci E (1984) Crystal-matrix relationships in calcifying organic matrices. INSERM 125:459–472

Boyde A (1964) The structure and development of mammalian enamel. PhD thesis. University of London, London

Bringas P, Nakamura M, Nakamura E, Evans J, Slavkin HC (1987) Ultrastructural analysis of enamel formation during in vitro development using chemically-defined medium. Scann Micr 1:1103–1108

Deutsch D (1989) Structure and function of enamel gene products. Anat Rec 224:189–210

Diekwisch T, David S, Bringas P, Santos V, Slavkin HC (1993) Antisense inhibition of AMEL translation demonstrates supramolecular controls for enamel HAP crystal growth during embryonic mouse molar development. Development 117:471–482

Doi Y, Eanes ED, Shimokawa H, Termine JD (1984) Inhibition of seeded growth of enamel apatite crystals by amelogenin and enamelin proteins in vitro. J Dent Res 63:98–105

Eanes ED (1973) Amorphous intermediates in the formation of biological apatites. In: Physico-Chimie et Cristallographie des Apatites d'intérét biologique. Colloques internationaux du centre national de la recherche scientifique 230, Paris, pp 296–301

Eanes ED, Termine JD, Nylen MU (1973) An electron microscopic study of the formation of amorphous calcium phosphate and

its transformation to crystalline apatite. Calc Tiss Res 12:143–158

Evans J, Bringas P, Nakamura M, Nakamura E, Santos V, Slavkin HC (1988) Metabolic expression of intrinsic developmental programs for dentine and enamel biomineralization in serumless, chemically-defined, organotypic culture. Calc Tiss Int 42:220–230

Fearnhead RW (1979) Matrix-mineral relationships in enamel tissues. J Dent Res 58B:909–916

Fincham, AG, Hu Y, Lau EC, Slavkin H, Snead ML (1991). Amelogenin post-secretory processing during biomineralization in the postnatal mouse molar tooth. Archs Oral Biol 36.305–317

Fincham AG, Lau EC, Simmer J, Zeichner-David M (1992) Amelogenin biochemistry – form and function. In: Slavkin H, Price P (eds) Chemistry and Biology of Mineralized Tissues. Elsevier, Amsterdam, pp 187–201

Frank RM, Sognnaes RF, Kerns R (1960) Calcification of dental tissues with special reference to enamel ultrastructure. In: Calcification in Biological Systems. AAAS, Washington DC, pp 163–202

Glimcher MJ (1979) Phosphoproteins of enamel. J Dent Res 58B: 790–806

Goodman AH, Martinez C, Chavez A (1991) Nutritional supplementation and the development of linear hypoplasias in children from Texonteopan, Mexico. Am J Clin Nutr 53:773–781

Haeckel E (1866) Generelle Morphologie der Organismen. Allgemeine Grundzüge der organischen Formen-Wissenschaft, mechanisch begründet durch die von Charles Darwin reformierte Descendenz-Theorie, 2 vols. George Reimer, Berlin, vol 2, p 300

Hayashi Y, Bianco P, Shimokawa H, Termine JD, Bonucci E (1986) Organic-inorganic relationships, and immunohistochemical localization of amelogenins and enamelins in developing enamel. Basic Appl Histochem 30:291–299

Heughebaert JC, Montel G (1973) Sur la transformation des phosphates amorphes en phosphates apatitiques par reaction intracristalline. Coll Int CNRS 283–293

Höhling HJ (1966) Die Bauelemente von Zahnschmelz und Dentin aus morphologischer, chemischer und struktureller Sicht. Carl Hanser, Munich

Höhling H, Barckhaus RH, Krefting ER, Althoff J, Quint P, Niestadtkötter R (1981) Relationship between the Ca-phosphate crystallites and the collagen structure in turkey tibia tendon. In: Veis A (ed) The Chemistry and Biology of Mineralized Tissues. Elsevier, Amsterdam, pp 113–117

Infante PF, Gillespie M (1977) Enamel hypoplasia in relation to caries in Guatemalan children. J Dent Res 56:493–498

Johnsson MSA, Nancollas GH (1992) The role of brushite and octacalcium phosphate in apatite formation. Crit Rev Oral Biol Med 3:61–82

Kallenbach E (1971) Electron microscopy of the differentiating rat incisor ameloblast. J Ultrastruct Res 35:508–515

Kallenbach E (1982) Fine structure of extracted rat incisor enamel. J Dent Res 61:1515–1523

Kallenbach E (1986) Crystal-associated matrix components in rat incisor enamel. Cell Tissue Res 246:455–461

Landis WJ (1985) Temporal sequence of mineralization in calcifying turkey tendon. In: Butler WT (ed) The Chemistry and Biology of Mineralized Tissues. EBSCO Media, Birmingham, ALa., pp 497–500

Landis WJ (1986) A study of calcification in the leg tendons from the domestic turkey. J Ultrastruct Res 94:217–238

Landis WJ, Glimcher MJ (1982) Electron optical and analytical observations of rat growth plate cartilage prepared by ultracryomicrotomy: the failure to detect a mineral phase in matrix vesicles and the identification of heterodisperse particles as the initial solid phase of calcium phosphate deposited in the extracellular matrix. J Ultrastruct Res 78:227–268

Landis WJ, Burke GY, Neuringer JR, Paine MC, Nanci A, Bai P, Warshawsky H (1988) Earliest enamel deposits of the rat incisor examined by electron microscopy, electron diffraction, and electron probe microanalysis. Anat Rec 220:233–238

Landis WJ, Hodgens K, Song MJ, Arena J, Kiyonaga S, McEwen B (1992) Mineral and collagen interaction during calcification. In: Slavkin H, Price P (eds) Chemistry and Biology of Mineralized Tissues. Elsevier, Amsterdam, pp 211–219

Lee DD, Landis WJ, Glimcher MJ (1986) The solid calciumphosphate mineral phases in embryonic chick bone characterized by high voltage electron diffraction. J Bone Min Res 1:425–432

Lehner J, Plenk H (1932) Die Zähne. In: Stöhr, v. Möllendorf (eds) Handbuch der mikroskopischen Anatomie V/3. Springer, Berlin, p 570

Limeback H (1991) Molecular mechanisms in dental hard tissue mineralization. Curr Opinion Dent 1:826–835

Nanci A, Bringas P, Samuel N, Slavkin HC (1983) Selachian tooth development: III. Ultrastructural features of secretory amelogenesis in *Squalus acanthias*. J Craniofac Gen Dev Biol 3:53–73

Nanci A, Bendayan M, Slavkin HC (1985) Enamel protein biosynthesis and secretion in mouse incisor secretory ameloblasts as revealed by high resolution immunocytochemistry. J Histochem Cytochem 33:1153–1160

Nancollas GH (1979) Enamel apatite nucleation and crystal growth. J Dent Res 58B:861–869

Nancollas GH (1989) In vitro studies of calcium phosphate crystallization. In: Mann S, Webb J, Williams RJP (eds) Biomineralization. Chemical and Biochemical Perspectives. VCH, Weinheim, pp 157–187

Nelson DGA, Barry JC (1989) High resolution electron microscopy of nonstoichiometric apatite crystals. Anat Rec 224:265–276

Newesely H (1973) Epitaxy problems in biocrystalline ultra textures. In: Physico-Chimie et Cristallographie des Apatites d'intérét biologique. Colloques internationaux du centre national de la recherche scientifique 230, Paris, pp 203–209

Reith EJ (1960) The ultrastructure of ameloblasts from the growing end of rat incisors. Arch Oral Biol 2:253–262

Reith EJ (1967) The early stage of amelogenesis as observed in molar teeth of young rats. J Ultrastruct Res 17:503–526

Robinson C, Kirkham J, Briggs HD, Atkinson PJ (1982) Enamel proteins: from secretion to maturation. J Dent Res 61:1490–1495

Roennholm E (1962) The amelogenesis of human teeth as revealed by electron microscopy. II. The development of the enamel crystallites. J Ultrastruct Res 6:249–303

Slavkin HC (1973) The isolation and characterization of calcifying and non-calcifying matrix vesicles from dentine. In: Physico-Chimie et Cristallographie des Apatites d'intérét biologique. Colloques internationaux du centre national de la recherche scientifique 230, Paris, pp 162–177

Slavkin HC, Mino W, Bringas P (1976) The biosynthesis and secretion of precursor enamel protein by ameloblasts as visualized by autoradiography after tryptophan administration. Anat Rec 185:289–312

Smales FC (1975) Structural subunit in prisms of immature enamel. Nature 258:772–774

Thompson SW, Hunt RD (1966) Histochemical procedures: Von Kossa staining for calcium. In: Selected Histochemical and Histopathological Methods. Thomas, Springfield, Illinois, pp 581–584

Travis DF, Glimcher MJ (1964) The structure and organization of, and the relationship between the organic matrix and the inorganic crystals of embryonic bovine enamel. J Cell Biol 23:447–497

Warshawsky H (1989) Organization of crystals in enamel. Anat Rec 224:242–262

Wuthier R (1992) Matrix vesicles: formation and function – mechanisms in membrane/matrix-mediated mineralization. In: Slavkin H, Price P (eds) Chemistry and Biology of Mineralized Tissues. Elsevier, Amsterdam, pp 143–152

Yamada M, Bringas P, Grodin M, MacDougall M, Cummings E, Grimmett J, Weliky B, Slavkin HC (1980) Chemically defined organ culture of embryonic mouse tooth organs: morphogenesis, dentinogenesis, and amelogenesis. J Biol Buccale 8:127–139

Yamauchi M, Chandler GS, Katz EP (1992) Collagen cross-linking and mineralization. In: Slavkin H, Price P (eds) Chemistry and Biology of Mineralized Tissues. Elsevier, Amsterdam, pp 39–46

Yanagisawa T, Sawada T, Miake Y, Shimokawa H, Takuma S (1989) Immunocytochemistry of amelogenin and enamelin in vinblastine-treated rat-incisor ameloblasts and enamel. In: Fearnhead RW (ed) Tooth Enamel V. Florence Publishers, Yokohama, pp 181–185

Young RA (1973) Some aspects of crystal structural modeling of biological apatites. In: Physico-Chimie et Cristallographie des Apatites d'intérét biologique. Colloques internationaux du centre national de la recherche scientifique 230, Paris, pp 21–39